Synthesis, Purification and Surface Chemistry Study of α-Synuclein (61-95)

by

Saad Alrashdi

A Thesis Submitted in Partial Fulfillment

of the Requirements for the Degree of

Master of Science in Chemistry

Middle Tennessee State University

August 2018

Thesis Committee:

Dr. Chengshan Wang, Thesis Advisor

Dr. Jing Kong, Thesis Committee

Dr. Mengliang Zhang, Thesis Committee

ACKNOWLEDGEMENTS

In the last two years, I have experienced many interesting activities while interacting with people from diverse backgrounds including faculty staff and peers. Through such experiences, I have learnt many things due to the richness of the information offered by these people. I could not have made it without a word of advice from my faculty peers and staff. They always provided another dimension that enabled me to learn new things in academics as well as in life. I cannot forget the guidance of my lab partners who made the learning experience fruitful by providing deeper insights into our curriculum. I will always cherish our interaction that made my life in the university better.

I would like to recognize the efforts of my supervisors Dr. Chengshan Wang who provided the guidance which I needed in terms of technical and soft skills. I can only describe them as the go to people in times of doubt and in times when I needed inspiration. The time that my supervisors afforded me can not be repaid. Moreover, I would like to thank Dr. Jing Kong, and Dr. Mengliang Zhang for enabling me to navigate through the process of conducting my final year research. They enabled me to get the best out of my abilities by discovering my strengths and helping me overcome my weaknesses.

Also, I would like to acknowledge my family, friends, and colleagues who helped me throughout the study. Special thanks to my parents who were always there to support me morally, financially and spiritually. Their encouragement has brought me this far and this is the reason I will forever be indebted to them.

ABSTRACT

Parkinson's disease is the second most common neurodegenerative disease and is characterized by a progressive loss of the dopaminergic neurons in *substantia nigra*. The degenerating dopaminergic neurons develop a hallmark deposition of Lewy bodies comprising abundant abnormal aggregates (i.e., fibrils) of α-synuclein (α-syn), which is a protein contains 140 amino acid residues.[1] Despite the abundance (~1% among the total proteins) in the brain, α-syn accumulates in the presynaptic terminals where exists high concentration of amphiphilic structure (e.g., lipsomes and cell membrane) and the reason of the accumulation is not clear. α-Syn was shown to be able to form a stable Langmuir monolayer at the air-water interface by Langmuir technique, which utilizes air-water interface to mimic the amphiphilic structure in vivo. From circular dichoism and FTIR results, α-syn was found to transform from unstructured conformation in aqueous solution to α-helix at the interface. Because α-helix is stable at the interface, this transformation explains the reason of the accumulation of α-syn around the amphiphilic structure.[2] On the other hand, the primary structure of α-syn constitutes three domains: N-terminal residues 1–60; the nonamyloid component (NAC) which spans residues 61–95 and is responsible for the aggregation; and residues 96–140 which comprise the negatively charged C-terminus.[3] In this thesis, α-syn(61-95) was synthesized and purified. In addition, α-Syn(61-95) was shown to also form a stable Langmuir monolayer at the air-water interface.

TABLE OF CONTENTS

LIST OF FIGURES

LIST OF SCHEMES

Chapter 1 Introduction

1.1 Parkinson's disease

Parkinson's disease (PD) is the second most common neurodegenerative disease (next only to Alzheimer's disease), affecting more than 1% of the people over the age of 65 in the United States.[1] Past clinical research has found a number of pathologic features in the PD-afflicted brain. PD is characterized by a progressive loss of the dopaminergic neurons in the *substantia nigra*.[2-5] The degenerating dopaminergic neurons develop a hallmark deposition of Lewy bodies (LB) comprising abundant α-synuclein (α-syn) fibrils.[6,7] Despite the extensive efforts to understand and prevent the PD pathogenesis, there is presently no cure for PD and available treatments offer only symptomatic relief to PD patients.

1.2 α-Synuclein

Various hypotheses, the majority of which invoke a role of α-syn, have been proposed to explain the etiology of PD. α-syn is a 140-amino-acid presynaptic protein whose function is not known.[8] The primary structure of α-syn (Scheme 1) constitutes three domains: residues 1–60 which are rich in positively charged lysine residues and contains four 11-amino acid imperfect repeats; the nonamyloid component (NAC) which spans residues 61–95 and is highly amyloidogenic; and residues 96–140 which comprise the negatively charged C-terminus.[8] One hypothesis suggests that the natively unstructured α-syn molecules misfold to form various aggregates in the cytoplasm of dopaminergic cells under adverse conditions.[9,10] Such aggregates may

deposit onto cell membranes, creating ion channels (pores) that lead to neuronal cell death.[9,11-13]

MDVFMKGLSK AKEGVVAAAE KTKQGVAEAA GKTKEGVLYV GSKTKEGVVH GVATVAEKTK EQVTNVGGAV VTGVTAVAQK TVEGAGSIAA ATGFV*KKDQL GKNEEGAPQE GILEDMPVDP DNEAYEMPSE EGYQDYEPEA*

Scheme 1. The sequence of α-synuclein with the N-terminus underlined and the C-terminus expressed in Italics.

1.3 Conformation change of α-syn

Momomeric α-syn is unstructured in aqueous solution, in which it can gradually form aggregates which are in β-sheet conformation. As shown by in vitro studies, the mature fibrils identical to those detected in Lewy bodies.[8,14,15] Thus, the aggregation procedure of α-syn has been studied extensively in aqueous solution. Notice that it has been shown that α-syn in the presence of vesicles adopts the α-helical conformation.[16,17] Because in vivo α-syn is found to be enriched near the presynaptic terminals (PST) of neuron,[18] where exists abundant vesicles.[19] Therefore, among the various factors effecting the misfolding and aggregation of α-syn, lipid bilayers (e.g., cell membrane and vesicle) have attracted extensive attention.[10,17] However, the structure of lipid bilayers is complicated and discussed as below.

1.4 Three regions of the structure of lipid bilayers

The structure of lipid bilayers can be divided into three regions as following: [20] i) the interior core of the membrane, which has a hydrophobic character; ii) the hydrophilic headgroups of the lipids; iii) the lipid-water interfacial layer (LWIL) at which the dielectric permittivity is much smaller than the bulk of the cell matrix.[21,22] The three regions stay together and cannot be separated. Thus, it is difficult to determine which layer induces the conformation change of α-syn. Interestingly, the air-water interface has been well accepted as a simple and excellent mimicry of the lipid-water interfacial layer due to the similar dielectric constant between them.[23] Compared with phospholipid bilayer structures, the physical parameters (such as distance between molecules and surface pressure which describes the interaction between molecules) of the air-water interface can be more easily monitored by Langmuir monolayer technique as shown below..

1.5 Langmuir monolayer technique

The measurement of Langmuir monolayer is accomplished by an instrument called a Langmuir trough, which is diagramed in Scheme 2. A Langmuir trough consists of a rectangular trough which contains the solution, which is called the subphase with the edges of the exposed surface surrounded by hydrophobic barriers polytetrafluoroethylene. Molecules which may form a LM are deposited on the surface with a syringe. The two shorter sides of the rectangular surface may be mechanically compressed, and the Langmuir monolayer will be trapped between the barriers. Because both the available surface area and amount of substance deposited on the surface is

known, the distance between the molecules at the surface can be described by area per molecule (or molecular area). As the molecular area decreases, the molecules will be compressed together. This compression will result in molecular interactions, which increase the surface pressure of the interface to which the molecules are confined. This increase in surface pressure is detected by an inert probe which contacts, but does not significantly penetrate, the surface of the air-water interface via the decreasing tension it exerts on a mass balance from which it hangs. It is worth noting that spectroscopic methods can be combined with Langmuir monolayer technique to elucidate the structure of the monolayer. Infrared Reflection-Absorption spectroscopy (IRRAS) is one of the most important spectroscopic methods mentioned above and the theory of IRRAS is below.

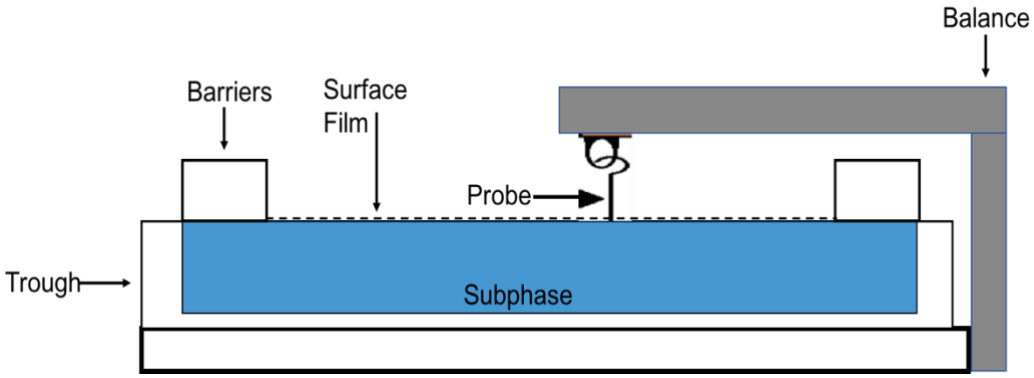

Scheme 2. Langmuir trough diagram.

1.6 IRRAS

IRRAS involves reflecting the incident infrared (IR) light beam from a surface (e.g. the air-water interface) to study the orientation of various vibrations at the air-water interface. To study molecules at the interface, the

orientation of the polarity of the electric and magnetic field vectors of the incident IR light is controlled. Orienting the electric field vector (also called the p-vector) of the incident IR beam parallel to the normal of the air-water interfacial plane is called p-polarized IRRAS. A diagram of p-polarized IRRAS is given in Scheme 3. This type of IR spectroscopy will result in a characteristic absorption spectrum that changes with the orientation of the molecules at the interface around Brewster angle.[23]

If a vibration is parallel to the air-water interface, the peak will be negative first and changes to positive when the incident angle is bigger than Brewster angle. For the vibrations perpendicular to the interface, the peak pattern is reversed: the peak is positive when the incident angle is below Brewster angle and changes to negative above the Brewster angle. Molecules at the surface which have a random orientation relative to the air-water interface plane will not have significant peaks in the p-polarized IRRAS spectrum.[23] Water molecules, buffer salts, and randomly oriented surface species are not favored by the selection rules of p-polarized IRRAS.[23] This creates the advantage of eliminating IR spectral bands which may overlap those bands of interest, such as the O-H band of water overlaps the Amide I band of polypeptides. The Brewster angle is the angle of incidence at which no polarized light is reflected from the surface. This angle varies with the varying chemical makeup of the surface and it is 54.2° from the surface normal for water.[24] Thus, IRRAS is a very important method to provide orientation information of proteins/peptides at interface by the amide bands shown below.

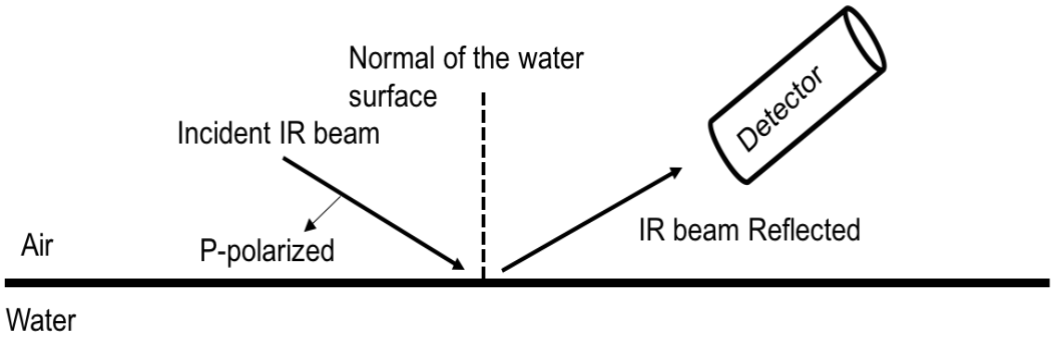

Scheme 3. Diagram of p-polarized IRRAS.

1.7 Amide bands of proteins/peptides

In FTIR spectroscopy, the amide functional group of the backbone of the polypeptide backbone absorbs infrared radiation, giving rise to nine characteristic 'Amide' IR bands namely Amide A, B, and I through VII.[23,25-28] Particularly, the Amide I band absorption ranges from 1600-1700 cm^{-1}, the C=O stretching vibrations of the amide carbonyl contributes around 85% to this band.[29] The position of amide I band is related to the secondary structure of proteins/peptides. For example, unstructured conformation shows a peak at ~1640 cm^{-1} for the Amide I band and the peak of β-sheet is ~1630 cm^{-1}. For α-helical segments, the peak position is significantly affected by the length of the helix. For a long helix, the peak will appear at ~1648 cm^{-1} and shifts to higher frequency as the helix becomes shorter.[29-31] All other amide bands are composed of overlapping frequencies of the vibrations of multiple functional groups and are not yet widely used for secondary structural studies. Together with FTIR, circular dichroism (CD) has been also used to confirm the secondary structure of proteins/peptides as the following.

1.8 CD spectroscopy

Due to the large amount of carbonyls (C=O which absorbs intensively around 200 nm) in the backbone amide bonds, proteins usually show strong CD signals between 260 and 180 nm.[23,26,28] Since the carbonyls are arranged differently in conformations (such as α-helix, β-sheets, and unstructured conformation), every secondary structure shows its distinct patterns in CD spectrum as below.[32,33] The α-helix conformation shows two characteristically negative peaks at 222 and 208 nm and one positive peak at 192 nm. The Far-UV CD of β-sheet conformation exhibits a positive peak at 196 nm and a negative peak at 215 nm. As for the unstructured conformation, only one negative peak at 199 nm will be detected. Surface chemistry technique (i.e., Langmuir monolayer technique) together with surface spectroscopic techniques (e.g., IRRAS and CD) has been used to elucidate both conformation and orientation of peptides at interface and provided helpful information for biophysics and biochemistry. A good example is the surface chemistry and surface spectroscopy study of α-syn.

1.9 Surface chemistry and surface spectroscopy study of α-syn

α-Syn was found to form a Langmuir monolayer at the air-water interface and the monolayer was found to be very stable.[23] As mentioned above in Section 1.2, α-syn in aqueous solution is in unstructured conformation which has never been reported to form a stable Langmuir monolayer. Thus, it is very interesting to study the conformation of α-syn at the air-water interface. The CD spectrum of quartz slides with the deposition of α-syn Langmuir monolayer showed two negative peaks at 222 and 208 nm and one positive peak at 192 nm, which is the characteristic peak ofα-helix. This indicates that

α-syn is in α-helix rather than unstructured conformation at the air-water interface. To further confirm this conclusion, the s-polarized IRRAS of α-syn detected the amide I band at 1655 cm^{-1}, which is clearly assigned to α-helix. As a consequence, the combination of Langmuir monolayer technique, CD, and IRRAS results clearly support the conclusion that the unstructured α-syn in aqueous solution transforms to α-helix when spread at the air-water interface. [23]

1.10 Thesis proposal

As mentioned in section 1.2, α-syn contains three regions: N-terminus (residues 1－60), NAC part (residues 61－95), and C-terminus (residues 96－140). Although the transformation of α-syn has been detected by the combination of surface chemistry and spectroscopy techniques above, which region is mainly responsible for the transformation has not been verified. In this thesis, the NAC part of α-syn, termed as α-syn (61－95) hereafter, is synthesized by Fmoc solid phase synthesis and purified by HPLC. It is worth noting that the N-terminus of a peptide can be capped with acetyl group and the C-terminus can be capped with ammonia group. To comprehensively examine the terminus effect, N-terminus α-syn (61－95) was capped by acetyl group to form N-capped α-syn (61－95) and both capped α-syn (61－95) was also synthesized by capping both N- and C-terminus. The aqueous solution of all the three types of α-syn (61－95) was spread at the air-water interface and all of them were found to be able to form a stable Langmuir monolayer. On

the other hand, the N-capped and both capped α-syn (61－95) showed a smaller molecular area than the uncapped α-syn (61－95) (which remains both N- and C-terminus naked). This difference may be explained by IRRAS in the future.

Chapter 2 Materials and methods

2.1 Solid phase peptide synthesis.

2.1.1 Uncapped α-syn (61－95) synthesis

The synthesis of uncapped α-syn (61－95) was performed through the solid-phase peptide synthesis using the microwave-assisted 9-fluorenylmethoxycarbonyl (Fmoc) peptide synthesis. Wang resin with 100-200 mesh beads of polystyrene polymer functionalized at a density of 0.7 mM/g with phydroxybenzyl alcohol groups to which the amino acid carboxyl attaches was used as the solid support.

The synthesis of the target peptide was performed from the C-terminus to N-terminus. The C-terminal residue was coupled to the resin by activating the carboxyl group on the free amino acid with diisopropylcarbodiimide (DIC), using hydroxybenzoyltriazole (HOBt) to suppress racemization in the first step of Fmoc-peptide synthesis. During this first coupling step in which the C-terminal amino acid is coupled to the resin in ten minutes, catalytic acceleration of the activation of the amino acid carboxyl was achieved by adding 0.2 molar equivalents to Wang resin of 4-dimethylaminopyridine (DMAP).

The reactants were agitated in dimethylformamide (DMF), which is the solvent for the coupling step for 5 minutes. The reactants were removed upon completion of the reaction by washing with DMF. The resin bound residues were deprotected through the suspension and agitation of the resin in a 1:4 Piperidine/DMF (v/v) solution for 3 minutes to enable it to react with the Fmoc

group. After removing the Fmoc protecting group via the procedure as described above, the resin-bound amino acid was ready for coupling to the next residue in the sequence, with the coupling time decreased to 3 minutes for all the remaining residues.

The residues in the sequence were linked to the Wang resin one by one by the circle of coupling-deprotection mentioned above. When the sequence is finished, the peptide was cleaved from the resin by adding 20 mL of trifluoroacetic acid (TFA)/DCM/triisopropylsilane/H_2O with a ratio of 75:22:1.5:1.5 (v/v). The cleavage cocktail was collected in a round bottom flask equipped with a stirrer and cooled in an ice-bath during the preparation. The cleavage mixture was filtered, and the resin rinsed with pure trifluoroacetic acid. The filtrate was slowly added to cool Methyl tert-butyl ether (8–10 mL ether/mL cleavage cocktail) and the precipitate left to settle and filtered off. The peptide was resuspended in the ether, stirred and left to settle in the cold. The peptide precipitated and the mixture was then centrifuged. After the supernatant was dumped away, the peptide was dried under vacuum for the HPLC purification

2.1.2 N-Capped synthesis

The protocol for the synthesis of N-uncapped α-syn (61—95) was the same as the one of the uncapped peptide, except the capping of the N-terminal residue which is the last in the sequence of the peptide. The capping was performed using acetyl anhydride together with the catalysis of pyridine to cap the naked amine (NH_2) in the N-terminus.

2.1.3 Both-capped α-syn (61－95) synthesis

The synthesis of Both-Capped α-syn (61－95) began with the Rink amide resin, and all of the other steps (such as coupling, deprotection, capping of N-terminus, and so on) are identical to the one of N-cappedα-syn (61－95).

2.2 Mass Spectrometry

Mass Spectrometry (MS) is used to measure the distribution of the molecular weight (MW) compounds in a sample. MS analysis was carried out on a Waters Synapt G2 Electrospray Ionization (ESI)-TOF mass spectrometer (Waters Corp., Milford, MA). Determination of the molecular weight is done through three basic steps namely ionization, acceleration of the ionized compounds towards the detector, and separation of the ions based on their mass to charge ration. In the first step, the sample molecules in the present experiment were ionized through electrospray ionization, which involves expelling the liquid sample from a small capillary to create an aerosol which is ionized by a coulombic charge on the capillary. The second step involved acceleration of the ionized molecules through an electric field gradient towards the detector. In the final step, the ions were separated by a mass analyzer based on their mass to charge ratio as they moved towards the detector. The magnetic field generated to separate the moving ions was achieved in this research by a Time of Flight (ToF) mass analyzer. α-Syn (61－95) product was dissolved in pure water and injected into the mass spectrometer to all for the analysis of the molecular weight of the ions in the

sample. The MS chromatogram was obtained at a capillary ionization voltage of 3.00 keV.

2.3 High-Performance Liquid Chromatography

Liquid chromatography is the most prominent separation technique used for non-volatile compounds. The separation of compounds is based on their affinity to the functionality of the surface of porous column material. The compounds' affinity is manipulated by controlling their solvents' concentration. Normal phase HPLC refers to the situation when the column material surface is functionalized with a hydrophilic functionality. However, reverse phase HPLC refers to functionalizing the column packing material with a hydrophobic functionality.

In the present research, HPLC was carried out on a Waters 1525 Binary Solvent Pump (Waters Corp., Milford, MA) attached to a Phenomenex Reverse Phase Semi Prep C18 Column (Model Jupiter-00G-4055- P0). Monitoring of UV absorbance at 200-250 nm was carried out to detect the molecule ions and measured by a waters 2489 UV-Vis detector (Waters Corp., Milford, MA). The mobile phase A used was water/0.1% TFA (v/v) while the mobile phase B was utilized by acetonitrile/0.1% TFA (v/v). α-Syn (61－95) molecules were separated from impurities by a linear gradient of 10-45% B at a flow rate of 21.2 mL/minute for 40 minutes. Through mass spectroscopy, the retention time of α-syn (61－95) moieties was able to be identified. Confirmation of the molecular weight of the α-syn (61－95) in the fraction was done by mass spectroscopy, after which the chromatography

was repeated. Lastly, the fractions obtained were frozen at -80 °C and lyophilized to obtain the solid purified α-syn (61—95).

2.4 Langmuir Trough π -A Isotherm

The surface pressure-area (π −A) isotherm of the Langmuir monolayer of α-syn(61—95) were conducted in a A Kibron μtrough (Kibron Inc., Helsinki, Finland). The water utilized as subphase (pH=5.5) for the monolayer study was obtained from a Modulab 2020 water purification system (Continental Water System Corp., San Antonio, TX) with a surface tension of 72.6 $mN \cdot m^{-1}$ and a specific resistivity of 18 MΩ·cm at 20.0 ± 0.5 °C. The concentration of the α-syn(61—95) aqueous solution was 0.225 mg/mL and 25 μL of the α-syn(61—95) solution were spread at the air-water interface, followed by a 30-min period for the monolayer formation. The compression rate was set at 50 $Å^2 \cdot molecule^{-1} min^{-1}$.

Chapter 3 Results

3.1 HPLC chromatogram of uncapped α-syn (61－95)

The HPLC chromatogram of uncapped α-syn (61－95) is shown in Figure 1. The wavelength of the UV absorption detector is set at 250 nm because of the characteristic UV absorption of the phenylalanine present in the sequence is around 250 nm. From the chromatogram, most of the major peaks are from impurities and the peak of uncapped α-syn (61－95) is at 21.5 minutes. The low intensity of this peak is due to two reasons. First, the extinction coefficient of phenylalanine at 250 nm is not so high. Second, there is only one phenylalanine in the sequence of α-syn (61－95). However, the eluant of at this retention time is confirmed to be α-syn (61－95) by Mass results shown below.

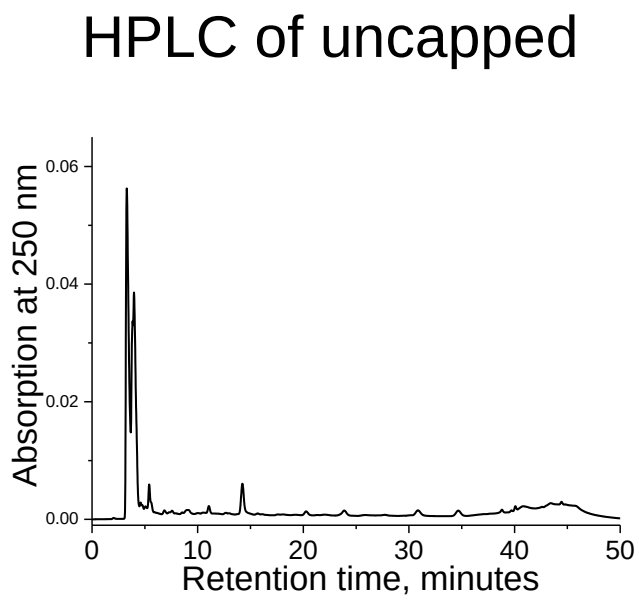

Figure 1. HPLC chromatogram of uncapped α-syn(61－95)

3.2 Mass spectrum of uncapped α-syn(61－95)

Figure 2 depicts the electrospray Mass spectra of the eluant with a retention time of 21.5 minutes in Figure 1. The peak appearing at 1631.95 is assigned to the diprotonated α-syn(61－95). The peaks at 1088.30 and 816.47 are due to the triple and quadruple protonated α-syn(61－95), respectively. According to the peaks above, the experimentally measured molecular weight of α-syn(61－95) is 3261.9 Da which is very close to theoretical value at 3260.6 Da. In addition, there is no other peaks of impurities detected in Figure 2. Consequently, the synthesis and purification of uncapped α-syn(61－95) is successful.

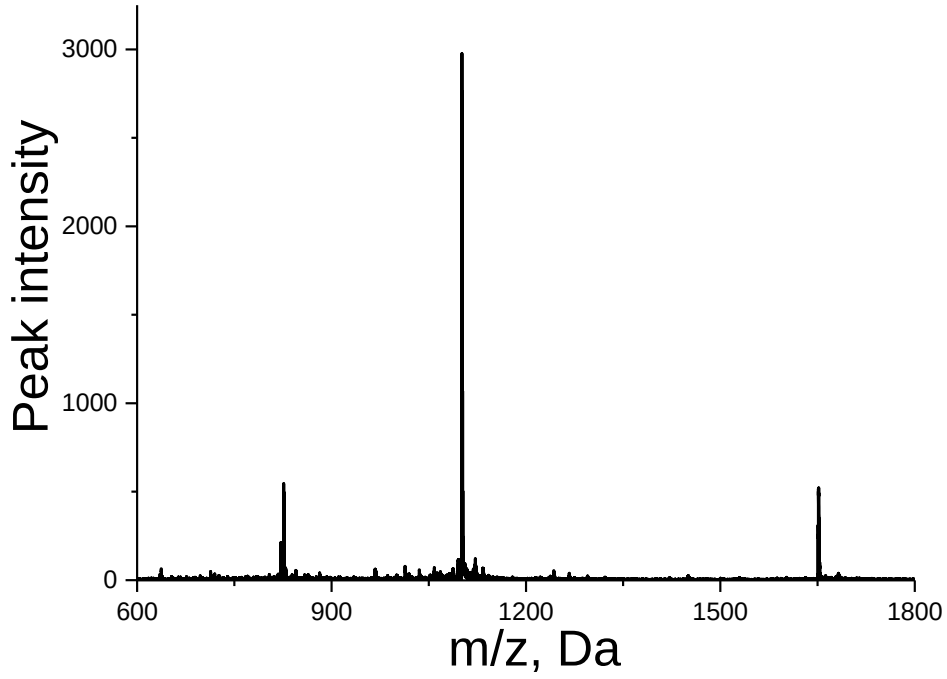

Figure 2. Mass spectrum of uncapped α-syn(61－95)

3.3 HPLC chromatogram of Both-capped α-syn(61－95)

The HPLC chromatogram of Both-capped α-syn(61－95) is shown in Figure 3. Similar to the result of uncapped α-syn(61－95) shown in Figure 1, most of the major peaks are from impurities and the peak of N-capped α-syn(61－95) is at 18.5 minutes (see the inset of Figure 3). Because reverse phase HPLC column was used during the purification, this indicates that the Both-capped α-syn(61－95) is more polar than the uncapped α-syn(61－95). Again, the eluant of at this retention time is confirmed to be Both-capped α-syn(61－95) by Mass results as the following.

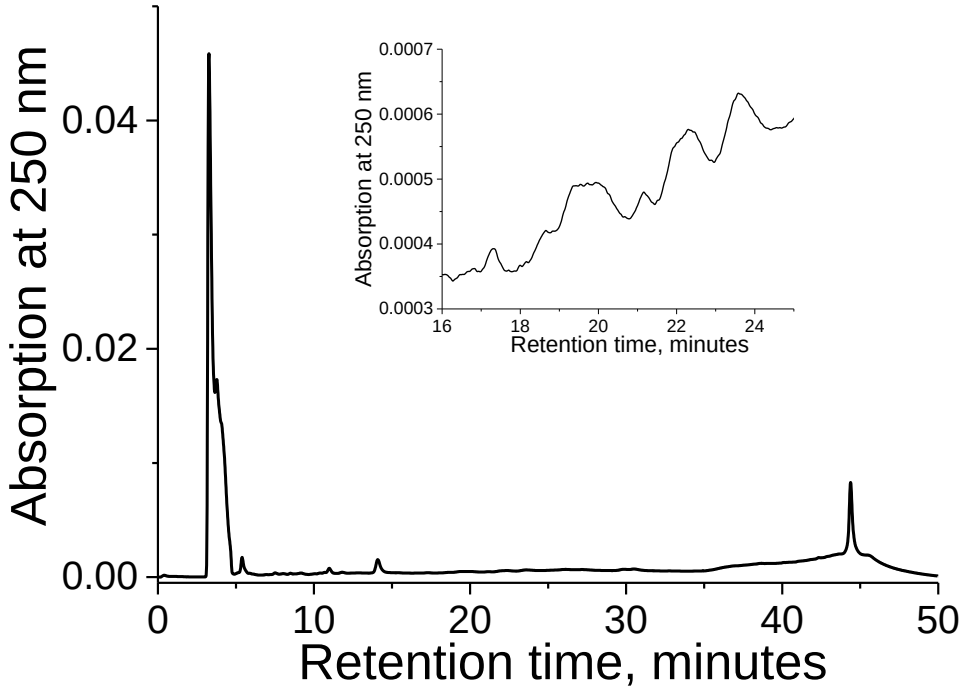

Figure 3. HPLC chromatogram of uncapped α-syn(61－95). Inset: Zoom in around the retention time of 20 minutes.

3.4 Mass spectrum of Both-capped α-syn(61－95)

Figure 4 depicts the electrospray Mass spectra of the eluant with a retention time of 18.5 minutes in Figure 2. The peak appearing at 1651.36 is assigned to the diprotonated α-syn(61－95). The peaks at 1101.23 and 826.18 are due to the triple and quadruple protonated α-syn(61－95), respectively. According to the peaks above, the experimentally measured molecular weight of α-syn(61－95) is 3300.7 Da which is also very close to theoretical value at 3301.1 Da. In addition, there is no other peaks of impurities detected in Figure 4. Consequently, the synthesis and purification of Both-capped α-syn(61－95) is also successful.

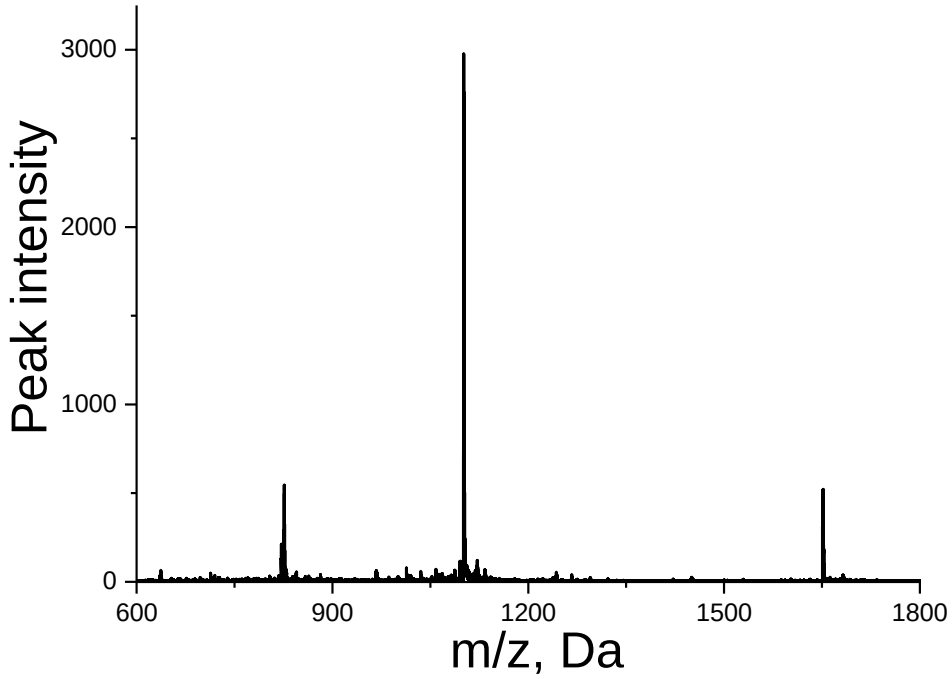

Figure 4. Mass spectrum of Both-capped α-syn(61－95)

3.5 HPLC chromatogram of N-capped α-syn(61－95)

The HPLC chromatogram of N-capped α-syn(61－95) is shown in Figure 5. Similar to the results shown in Figure 1 and 3, most of the major peaks are from impurities and the peak of N-capped α-syn(61－95) is also at 18.5 minutes (see the inset of Figure 5). This indicates that the polarity of N-capped α-syn(61－95) is similar to that of Both-capped one and stronger than that of the uncapped α-syn(61－95). Again, the eluant of at this retention time is confirmed to be Both-capped α-syn(61－95) by Mass results similar to Figure 4. Because the molecular weight of N-capped α-syn(61－95) is very similar to that of Both-capped one, the Mass result of N-capped α-syn(61－95) is not shown here.

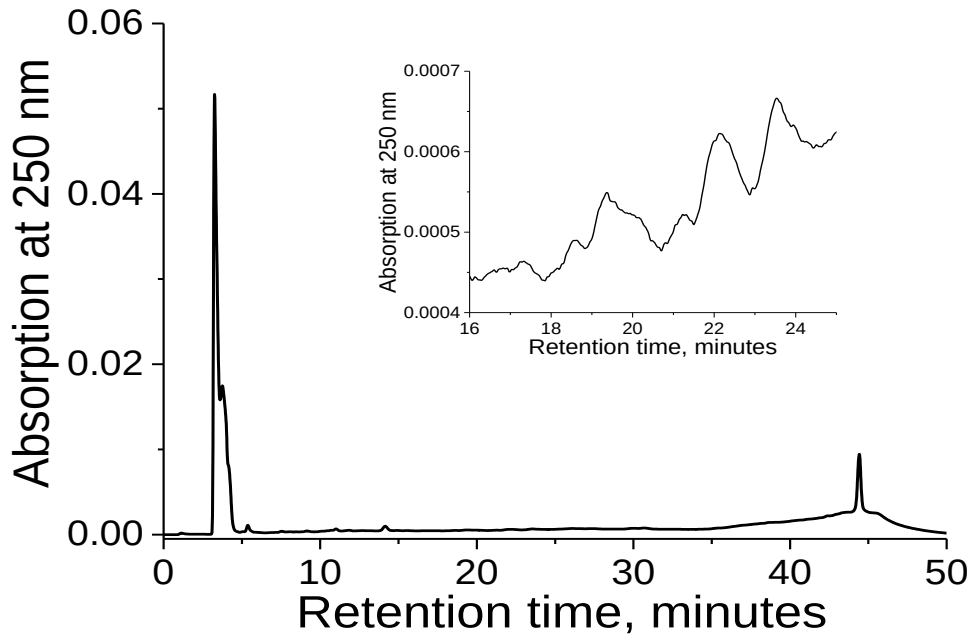

Figure 5. HPLC chromatogram of N-capped α-syn(61－95). Inset: Zoom in around the retention time of 20 minutes.

3.6 Surface chemistry of three types of α-syn(61－95)

The surface pressure-area (π－A) isotherms of all the three types of α-syn(61－95) are shown in Figure 6. The lift-off point of the π-A isotherm was situated at 400 Å^2/molecule, followed by a steady increase of the surface pressure up to a kink point at 360 Å^2/molecule. Decreasing the surface area further caused the surface pressure to increase quickly and the collapse was observed at 205 Å^2/molecule with a surface pressure at 17 mN/m． The limiting molecular area was obtained at 350 Å^2/molecule by extrapolating the higher surface pressures of the isotherm to nil surface pressure. As suggested in section 3.3 and 3.5, the N-capped and Both-capped α-syn(61－95) are more polar than uncapped α-syn(61－95). Therefore, it is not a surprise that the limiting molecular area of N-capped and Both-capped α-syn(61－95) are at 240 and 245 Å^2/molecule, respectively.

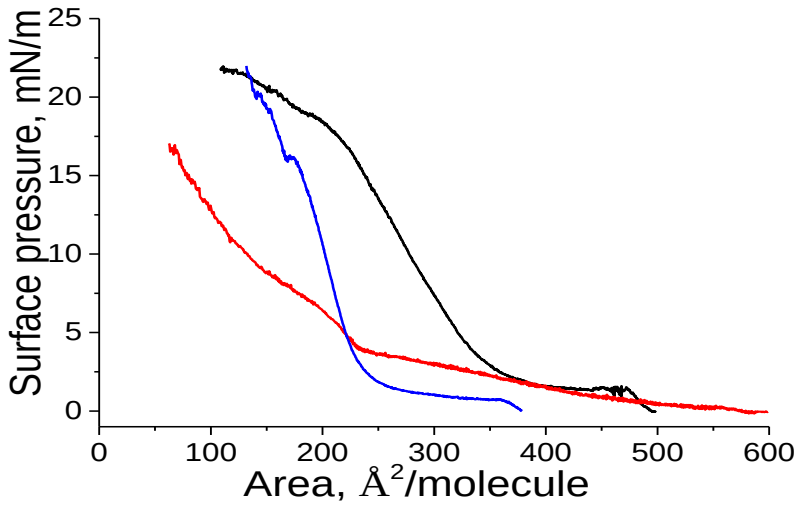

Figure 6. π－A isotherms of uncapped (black), N-capped (red), and Both-capped (blue) α-syn(61－95) when pure water was used as subphase.

3.7 Conclusions

All the uncapped, N-capped, and Both-capped α-syn(61－95) have been synthesized and purified. In addition, all the three types of α-syn(61－95) can form stable Lanmguir monolayer structure at the air-water interface. The uncapped α-syn(61－95) showed a bigger limiting molecular area than that of N-capped or Both-capped α-syn(61－95). Together with the longer retention time of uncapped α-syn(61－95) than that of N-capped or Both-capped α-syn(61－95) in the reverse phase HPLC, the uncapped α-syn(61－95) is shown to be less polar than the other two. Usually, the naked amine (NH_2) group in the naked N-terminus of uncapped α-syn(61－95) is more polar than acetyl amide group (CH_3-CO-NH_2) in the N-capped or Both-capped α-syn(61－95). The reason why N-capped and Both-capped α-syn(61－95) is more polar than the uncapped α-syn(61－95) is still unknown and will be elucidated in the future work in the following Chapter.

Chapter 4. Future Work

As concluded above, all of the three types of α-syn(61－95) can form a stable Langmuir monolayer. However, the reason why they can form the monolayer is not clear. For example, to the best of our knowledgement, proteins/peptides in unstructured conformation have not been reported to be able to form a stable Langmuir monolayer. Thus, all of the three types of α-syn(61－95) may be in the α-helical conformation at the air-water interface. On the other hand, α-syn has been widely shown to be unstructured in aqueous solution. Similarly, all the three types of α-syn(61－95) may be also unstructured in aqueous solution before spread at the air-water interface. As a consequence, the α-syn(61－95) may also change its unstructured conformation in the aqueous solution to α-helix at the air-water interface. To detect this conformation change, CD will be used and a single negative peak at 199 nm is expected for the aqueous solution of α-syn(61－95). As for the Langmuir monolayer of α-syn(61－95), two negative peaks at 208 and 222 nm together with a positive peak at 192 nm are expected.

In addition, although there is only minor difference between the N-capped and uncapped α-syn(61－95), the difference between the limiting molecular area of them is substantial. The most probable reason is the tilted angle of the axis of α-helix of N-capped and uncapped α-syn(61－95). The axis of the uncapped α-syn(61－95) may be more parallel to the air-water interface whereas the N-capped one may be more tilted. The tilted angle of the axis of

the α-helices of N-capped and uncapped α-syn(61－95) can be evaluated by p-polarized IRRAS as mentioned in Chapter 1.

Notice that the limiting molecular area between the N-capped and Both-capped α-syn(61－95) is minor. Therefore, the N-terminus affects the polarity and the limiting molecular area more than the C-terminus. Isotopic labeling (such as ^{13}C or ^{15}N) will be introduced into the N-terminus to generate a new band in FTIR and IRRAS can provide more information about the important role of N-terminus including the acetyl cap in the behavior of α-syn(61－95).

Chapter 5 References

(1) www.michaeljfox.org/living aboutParkinsons parkinsons101.cfm.

(2) Forman, M. S.; Lee, V. M. Y.; Trojanowski, J. Q. *Neuron* **2005**, *47*, 479.

(3) Moore, D. J.; West, A. B.; Dawson, V. L.; Dawson, T. M. *Annu. Rev. Neurosci.* **2005**, *28*, 57.

(4) Dalfo, E.; Portero-Otin, M.; Ayala, V.; Martinez, A.; Pamplona, R.; Ferrer, I. *J. Neuropathology Exp. Neurol.* **2005**, *64*, 816.

(5) Chinta, S. J.; Andersen, J. K. *Int. J. Biochem. Cell Biol.* **2005**, *37*, 942.

(6) Spillantini, M. G.; Crowther, R. A.; Jakes, R.; Hasegawa, M.; Goedert, M. *Proc. Natl. Acad. Sci. U. S. A.* **1998**, *95*, 6469.

(7) Spillantini, M. G.; Schmidt, M. L.; Lee, V. M. Y.; Trojanowski, J. Q.; Jakes, R.; Goedert, M. *Nature* **1997**, *388*, 839.

(8) Wright, J. A.; Brown, D. R. *J. Neurosci. Res.* **2008**, *86*, 496.

(9) Caughey, B.; Lansbury, P. T. *Ann. Rev. Neurosci.* **2003**, *26*, 267.

(10) Fink, A. L. *Acc. Chem. Res.* **2006**, *39*, 628.

(11) Kostka, M.; Hogen, T.; Danzer, K. M.; Levin, J.; Habeck, M.; Wirth, A.; Wagner, R.; Glabe, C. G.; Finger, S.; Heinzelmann, U.; Garidel, P.; Duan, W.; Ross, C. A.; Kretzschmar, H.; Giese, A. *J. Biol. Chem.* **2008**, *283*, 10992.

(12) Lashuel, H. A.; Petre, B. M.; Wall, J.; Simon, M.; Nowak, R. J.; Walz, T.; Lansbury, P. T. *J. Mol. Biol.* **2002**, *322*, 1089.

(13) Volles, M. J.; Lansbury, P. T. *Biochemistry* **2002**, *41*, 4595.

(14) Qin, Z.; Hu, D.; Han, S.; Hong, D.; Fink, A. L. *Biochemistry* **2007**, *46*, 13322.

(15) Dusa, A.; Kaylor, J.; Edridge, S.; Bodner, N.; Hong, D.; Fink, A. L. *Biochemistry* **2006**, *45*, 2752.

(16) Borbat, P.; Ramlall, T. F.; Freed, J. H.; Eliezer, D. *J. Am. Chem. Soc.* **2006**, *128*, 10004.

(17) Zhu, M.; Fink, A. L. *J. Biol. Chem.* **2003**, *278*, 16873.

(18) Beyer, K. *Acta Neuropathol.* **2006**, *112*, 237.

(19) Yang, G.; Dong, Y.; Gong, K.; Jiang, W.; Kwon, E.; Wang, P.; Zheng, H.; Zhang, X.; Gan, W.; Zhao, N. *Neurosci. Lett.* **2005**, *384*, 66.

(20) Munishkina, L. A.; Phelan, C.; Uversky, V. N.; Fink, A. L. *Biochemistry* **2003**, *42*, 2720.

(21) Cherepanov, D. A.; Feniouk, B. A.; Junge, W.; Mulkidjanian, A. Y. *Biophys. J.* **2003**, *85*, 1307.

(22) Jiang, D.; Dinh, K. L.; Tuthenburg, T. C.; Zhang, Y.; Su, L.; Land, D. P.; Zhou, F. *J. Phys. Chem. B* **2009**, *113*, 3160.

(23) Wang, C.; Shah, N.; Thakur, G.; Zhou, F.; Leblanc, R. M. *Chem. Commun.* **2010**, *46*, 6702.

(24) Hasegawa, T.; Nishijo, J.; Watanabe, M.; Umemura, J.; Ma, Y.; Sui, G.; Huo, Q.; Leblanc, R. M. *Langmuir* **2002**, 4758.

(25) Dziri, L.; Desbat, B.; Leblanc, R. M. *J. Am. Chem. Soc.* **1999**, *121*, 9618.

(26) Wang, C.; Micic, M.; Ensor, M.; Daunert, S.; Leblanc, R. M. *J. Phys. Chem. B* **2008**, *112*, 4146.

(27) Jiang, D.; Men, L.; Wang, J.; Zhang, Y.; Chickenyen, S.; Wang, Y.; Zhou, F. *Biochemistry* **2007**, *46*, 9270.

(28) Wang, C.; Zheng, J.; Zhao, L.; Rastogi, V. K.; Shah, S. S.; DeFrank, J. J.; Leblanc, R. M. *J. Phys. Chem. B* **2008**, *112*, 5250.

(29) Dziri, L.; Desbat, B.; Leblanc, R. M. *J. Am. Chem. Soc.* **1999**, *121*, 9618.

(30) Belbachir, K.; Lecomte, S.; Ta, H. P.; Petibois, C.; Desbat, B. *Anal. Bioanal. Chem.* **2011**, *401*, 3263.

(31) Decatur, S. M. *Biopolymers* **2000**, *54*, 180.

(32) Aronoff-Spencer, E.; Burns, C. S.; Avdievich, N. I.; Gerfen, G. J.; Peisach, J.; Antholine, W. E.; Ball, H. L.; Cohen, F. E.; Prusiner, S. B.; Millhauser, G. L. *Biochemistry* **2000**, *39*, 13760.

(33) Sreerama, N.; Woody, R. W. *Anal. Biochem.* **2000**, *282*, 252.